

## General Disclaimer

### One or more of the Following Statements may affect this Document

- This document has been reproduced from the best copy furnished by the organizational source. It is being released in the interest of making available as much information as possible.
- This document may contain data, which exceeds the sheet parameters. It was furnished in this condition by the organizational source and is the best copy available.
- This document may contain tone-on-tone or color graphs, charts and/or pictures, which have been reproduced in black and white.
- This document is paginated as submitted by the original source.
- Portions of this document are not fully legible due to the historical nature of some of the material. However, it is the best reproduction available from the original submission.

**NASA TECHNICAL  
MEMORANDUM**

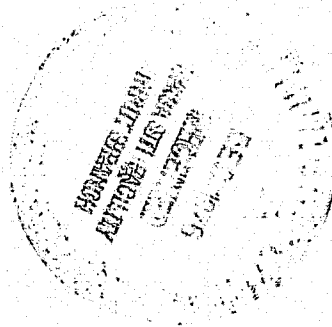
**NASA TM X-73559**

**NASA TM X-73559**

(NASA-TM-X-73559) INLET TOTAL PRESSURE LOSS  
DUE TO ACOUSTIC WALL TREATMENT (NASA) 16 p  
HC A02/MF A01 CSCL 01A

**N77-11991**

**G3/02    Unclass  
56902**



**INLET TOTAL PRESSURE LOSS DUE TO  
ACOUSTIC WALL TREATMENT**

by Brent A. Miller  
Lewis Research Center  
Cleveland, Ohio 44135

**TECHNICAL PAPER** to be presented at the  
Fifteenth Aerospace Sciences Meeting sponsored by the  
American Institute of Aeronautics and Astronautics  
Los Angeles, California, January 24-26, 1977

# INLET TOTAL PRESSURE LOSS DUE TO ACOUSTIC WALL TREATMENT

Brent A. Miller\*

National Aeronautics and Space Administration  
Lewis Research Center  
Cleveland, Ohio 44135

## Abstract

It was the purpose of the present investigation to determine experimentally the effect of diffuser wall acoustic treatment on inlet total pressure loss. Data were obtained by testing an inlet model with 10 different acoustically treated diffusers differing only in the design of the Helmholtz resonator acoustic treatment. Tests were conducted in a wind tunnel at forward velocities to 41 meters per second for inlet throat Mach numbers of .5 to .8 and angles of attack as high as 50 degrees. Results indicate a pressure loss penalty due to acoustic treatment that increases linearly with the porosity of the acoustic facing sheet. For a surface porosity of 14 percent the total pressure loss was 21 percent greater than that for an untreated inlet. The penalty resulting from treatment increased for average throat Mach numbers above approximately .7 where local regions of sonic or supersonic surface flow were encountered. Inlet performance at angle of attack was not significantly influenced by inlet acoustic treatment. Pressure loss over the treatment was not affected by the presence of noise generated by a siren even though sound pressure level measurements show the treatment reduced the siren noise by as much as 8 dB.

## Introduction

The addition of acoustic treatment to an engine inlet can be an effective method of suppressing engine machinery noise<sup>(1-3)</sup> in order to absorb acoustic energy the treatment surface must be porous. It has been shown<sup>(4)</sup> that this porosity will result in some increase in skin friction that will, in turn, lead to increased inlet total pressure loss. Thus the desire for inlet noise suppression will exact some penalty in inlet aerodynamic performance that will ultimately result in reduced engine thrust or increased fuel consumption. It was the purpose of the present investigation to determine experimentally the magnitude of this performance penalty in terms of inlet total pressure loss as a function of acoustic treatment design and inlet operating conditions. The author is not aware of any similar parametric experimental investigation defining the aerodynamic penalties of acoustic treatment in a flight type inlet.

The experimental results presented were obtained by testing inlets with 10 different acoustically treated diffusers and one baseline untreated (hard-wall) diffuser. All diffusers were of the same contour with a common entry lip

used for each inlet. Inlet overall proportions were those suitable for a high-subsonic cruise speed aircraft. Inlet overall length to diameter ratio was 1.0 with a diffuser area ratio of 1.1. The model inlet had a diffuser exit diameter of 30.48 centimeters (12 inches).

The acoustic treatment investigated was of the Helmholtz resonator type consisting of a perforated facing sheet over a honeycomb backing. Treatments tested differed in backing depth (.0075 to .0383 of diffuser exit diameter) and facing sheet porosity (2 percent to 14 percent open area). The treatment extended along the diffuser from slightly downstream of the throat to just upstream of the diffuser exit.

The tests were conducted in the Lewis Research Center's 2.74 by 4.58-meter (9x15 foot) Low Speed Wind Tunnel. A vacuum system was used in place of an engine or fan to induce inlet flow. A siren was used to simulate engine noise. Measurements were made of inlet total pressure loss, steady state total pressure distortion, surface Mach number distributions and noise suppression properties. Data were taken at wind tunnel flow velocities of 0 to 41 meters per second (0 to 80 knots) and angles of attack to as high as 50 degrees. Inlet average throat Mach number was varied over a range from .5 to in excess of .8.

## Symbols

$d$	diameter of hole in facing sheet
$D_c$	diameter of inlet centerbody
$D_e$	diffuser exit diameter
$D_{hl}$	inlet highlight diameter
$D_m$	inlet maximum outside diameter
$D_t$	inlet throat diameter
$\Delta p_{max}$	inlet total pressure distortion, [(maximum total pressure) - (minimum total pressure)] / (average total pressure)
$h$	depth of acoustical treatment honeycomb backing
$L$	length of inlet
$L_c$	length of inlet centerbody
$L_d$	length of diffuser
$M_s$	surface Mach number

\*Aerospace Engineer, Aeronautics Directorate

$\bar{M}_t$	throat Mach number determined from inlet mass flow and geometric throat area assuming one-dimensional flow
$P_\theta$	static pressure on inlet lip
$P_d$	total pressure at diffuser exit used to indicate flow separation
$P_o$	freestream total pressure
$P_1$	local total pressure at diffuser exit
$\bar{P}_1$	area averaged total pressure at diffuser exit
$\Delta P$	$P_o - \bar{P}_1$
$\bar{q}_t$	dynamic pressure corresponding to $\bar{M}_t$
$S$	axial length of acoustic treatment
$\Delta(\text{SPL})_{\text{BPF}}$	reduction in one-third-octave band sound pressure level at siren blade passing frequency, dB
$t$	thickness of acoustic facing sheet
$V_o$	freestream velocity
$x$	axial distance measured from highlight
$y$	radial position
$Y$	passage height
$\alpha$	angle of attack between freestream velocity vector and inlet centerline, deg.
$\alpha_{\text{sep}}$	angle of attack resulting in inlet flow separation
$\delta$	ratio of specific heats, equal to 1.4 for air
$\theta_m$	maximum diffuser wall angle, deg.
$\sigma$	percent open area of acoustic facing sheet

#### Test Apparatus

##### Facility

A schematic view of the test facility and model arrangement is shown in Figure 1. The tests were conducted in a 2.75- by 4.58-meter (9x15 foot) Low Speed Wind Tunnel at the Lewis Research Center. A vacuum system was used in place of a fan or compressor to induce inlet flow.

A venturi, calibrated in place against a standard ASME bellmouth, was used to measure inlet airflow. Inlet airflow was remotely varied using two flow control valves arranged to give both coarse and fine adjustment. Inlet

angle of attack was also remotely varied by means of the turntable on which the test apparatus was mounted. A swivel joint, containing a low-leakage seal, provided 360 degree rotation capability.

Inlet total pressure loss was computed at the diffuser exit (simulated fan face) using both hub and tip boundary layer rakes as well as total pressure rakes spanning the entire annulus. Eight full-span rakes were used with six equal-area-weighted tubes per rake. The eight hub and eight tip boundary layer rakes each contained 5 total-pressure tubes.

A siren, installed in the duct downstream of the inlet, was used as a noise source so that the effect of impressed noise on acoustic treatment pressure loss could be determined. The siren was in operation only when noise measurements were required and consequently was not used for most of the tests. Microphones, located in the wind tunnel upstream of the test section, were used to measure the acoustic suppression properties of each acoustic treatment design. A more complete description of the test facility can be found in reference 5.

##### Model Design

Inlet overall proportions and design are shown in Figure 2. These proportions were selected to be suitable for a high-subsonic cruise speed application. Design details of the removable, acoustically treated diffusers are shown in Figure 3. All ten acoustic treatments were of the Helmholtz resonator type consisting of a perforated facing sheet over honeycomb with a backing sheet attached to the honeycomb. The treatments differed only in facing sheet porosity,  $\sigma$ , and in the depth of the honeycomb,  $h$ . Facing sheet thickness,  $t$ , and hole diameter,  $d$ , were constant. Porosity of the facing sheet was varied by changing the number of holes per unit area.

The range of variables for the design of the acoustic treatment was influenced by an analysis of treatment acoustic properties. The model inlet was assumed to be scaled from a full size one for an engine with a fan diameter of approximately 1.7 meters and a blade passing frequency of about 900 Hertz. This resulted in a scaled blade passing frequency of 5000 Hertz for the models. Model treatment design was then varied parametrically about a design tuned for 5000 Hertz.

#### Results and Discussion

##### Basic Aerodynamic Performance

Surface Mach Number. The axial variation of surface Mach number within the inlet shown in Figure 4 gives an indication of the grazing flow and diffusion rates present over the acoustic treatment. The data shown were obtained at a freestream velocity of 41 meters per second and zero degrees angle of attack. The combined effects of surface curvature, and blockage due

to the spinner or centerbody, result in substantial diffusion occurring over the treatment. This complex distribution of surface Mach number, representative of a flight type inlet, would be impossible to duplicate with a simple test model employing straight or conical diffuser walls. Since the pressure loss over acoustic treatment will be influenced by the distribution of Mach number, the curved axisymmetric diffusers are necessary in order to obtain the proper grazing flow conditions.

**Sample Data.** Inlet total pressure loss,  $\Delta P$ , defined as the difference between the free-stream total pressure,  $P_0$ , and the area-averaged total pressure at the diffuser exit,  $\bar{P}_1$ , was determined for each diffuser over a range of inlet weight flows and angles of attack. Representative test results are shown in Figure 5 for the reference untreated, or hard-walled diffuser, and for the diffuser with 6.4 percent open area and a backing depth,  $h/D_0$ , of .015. The total pressure loss has been expressed in coefficient form by dividing the loss,  $\Delta P$ , by the dynamic pressure computed for a Mach number equal to the average throat Mach number,  $\bar{M}_t$ . Plots similar to this were prepared for each of the 10 treated diffusers and the data were then crossplotted to arrive at the results summarized in subsequent figures.

The relationship between the total pressure loss coefficient,  $\Delta P/\bar{q}_t$ , and total pressure recovery,  $\bar{P}_1/P_0$ , is shown by the graph of Figure 6. This figure was obtained by solving the appropriate isentropic compressible flow equations to yield:

$$\frac{\bar{P}_1}{P_0} = 1 - \left( \frac{\Delta P}{\bar{q}_t} \right) \left( \frac{\delta}{2} \right) \left( \bar{M}_t^2 \right) \sqrt{1 + \left( \frac{\delta-1}{2} \right) \bar{M}_t^2}^{\frac{\delta}{\delta-1}}$$

This figure, or the above equation, can be used to determine pressure recovery given the loss coefficient and the average throat Mach number. For example, from Figure 5, a maximum loss coefficient of approximately .04 was measured for throat Mach numbers below .7. Figure 6 then indicates that the pressure recovery for this data was greater than about .99. At higher average throat Mach numbers where the loss coefficient can increase 250 percent, to .1, the pressure recovery has dropped only 2 percent to approximately .97. This indicates that the absolute level of pressure loss due to the inlet was relatively small.

#### Effect of Sound Pressure Level

Tests were first conducted to determine if the presence or absence of impressed noise had any effect on inlet total pressure loss. This was accomplished by operating the treated inlets over a range of weight flows both with and without the siren noise source operating. Noise measurements were used to determine the acoustic effectiveness of the treatments by comparing the external sound pressure levels measured with the treated diffusers to the levels obtained with

the hard wall untreated one. The difference between these sound pressure levels, measured in the one-third-octave band containing the siren 5000-Hertz tone, is the sound pressure level reduction obtained with the acoustic treatment. The siren generated a sound pressure level in the inlet of approximately 145 dB at the diffuser exit.

Figure 7 shows the results of these tests where total pressure loss has been plotted versus sound pressure level reduction. The total pressure loss with the siren operating was divided by that obtained without the siren to more readily indicate any effect of impressed noise. The scattered nature of the data indicate no systematic affect of impressed noise on total pressure loss, even though the acoustic treatment reduced the siren tone sound pressure level by as much as 8 dB. The pressure loss in the boundary layer associated with the porous surface may have been sufficient to mask any additional pressure loss generated as a result of exciting the Helmholtz resonators. This lack of influence of sound pressure level on total pressure loss allowed subsequent tests, the results of which appear in the following sections, to be conducted without the siren operating.

#### Effect of Treatment Design

All data presented in this section were obtained at a freestream velocity of 41 meters per second and zero degrees angle of attack.

**Surface Porosity.** The increase in total pressure loss coefficient due to surface porosity is shown by the data of figure 8. Here the pressure losses measured with treated diffusers were divided by the loss with the untreated, or hard-wall diffuser, to obtain a direct measure of the additional loss resulting from the porous surface. The results shown were obtained by averaging the losses measured at average throat Mach numbers of .5, .6, and .7. Figure 5 shows the pressure loss coefficient to be approximately constant over this range of throat Mach number so that the data for each diffuser can be averaged to reduce data scatter and increase the confidence in showing the effect of surface porosity.

The data of Figure 8 show that the increase in pressure loss due to acoustic treatment is approximately linearly proportional to the porosity of the acoustic facing sheet. For example, using the dashed line drawn thru the data, a facing sheet porosity of 14 percent results in an increase in pressure loss of approximately 21 percent compared to the untreated inlet; whereas a penalty of 10 percent was measured for inlets with a porosity of 6.4 percent. This result suggests that the performance penalty due to acoustic treatment may be influenced by acoustic treatment design in a relatively simple systematic manner.

**Backing Depth.** Figure 9 presents pressure loss data as a function of acoustic treatment backing depth,  $h/D_e$ . This data is a re-plot of the data from the previous figure and shows no systematic effect of backing depth on pressure loss. This result was not unexpected and reflects the lack of flow within the honeycomb cells when the cell size is kept small, .95 cm. diameter for the present models, and when care is taken to seal the facing and backing sheets to the honeycomb so that flow between cells does not occur.

#### Effect of Operating Conditions

**Average Throat Mach Number.** The effect of average throat Mach number on inlet total pressure loss is shown in Figure 10, parts (a) thru (d), for each acoustic treatment as well as for the hard-wall diffuser. The pressure loss, plotted as a function of average throat Mach number, was normalized by the loss at  $M_e$  of .5 to more clearly show the effect of increasing Mach number. Data shown were obtained at zero angle of attack with a freestream velocity of 41 meters per second.

Figure 10 indicates that the loss coefficient is relatively constant for throat Mach numbers of .5 to .7. However, as the throat Mach number was increased above .7 all diffusers, including the hard-wall one, suffered a rapid increase in total pressure loss. Reference to Figure 4 indicates that this increase in loss coefficient occurs with the onset of locally sonic or supersonic flow near the inlet throat.

The increase in loss coefficient at higher throat Mach numbers was greater for the treated inlets than for the baseline hard-wall one. This indicates an additional adverse effect of wall acoustic treatment in the presence of sonic or supersonic diffusing flow over that present with a hard-wall. Also note that at higher throat Mach numbers the pressure loss appears to be influenced by backing depth and porosity. However, the effect is not systematic.

**Angle of Attack.** The effect on total pressure loss of increasing the angle of attack to 30 degrees is shown in figure 11. The pressure loss has been referenced to that measured at zero degrees angle of attack.

Figure 11(a) indicates that for an average throat Mach number of .5, total pressure loss increased approximately 10 percent when the angle of attack was increased to 30 degrees. With an increase in throat Mach number the penalty due to angle of attack at first decreased and then increased again for throat Mach numbers above approximately .60. Similar levels and trends can be seen in the data of parts (b), (c), and (d) of this figure.

Over the entire range of average throat Mach numbers the effect of increasing the angle of attack to 30 degrees on inlet total pressure loss was found to be essentially the same whether

the inlet contained acoustic treatment or not. The solid line shown on each part of Figure 11, obtained with the hard-wall diffuser, generally follows the same pattern of pressure loss as that shown for the treated diffusers. The reason for this behavior can be seen by examining total pressure profiles measured at the diffuser exit as a function of diffuser treatment design and angle of attack. Representative total pressure profiles shown in Figure 12 indicate that changing angle of attack has a much larger effect on total pressure than does the presence or absence of acoustic treatment. This large effect of angle of attack, for example, nearly a doubling of the loss at an average throat Mach number of .8 for the hard-wall diffuser, tends to mask any smaller effect due to acoustic treatment.

If angle of attack is increased sufficiently, inlet flow separation will occur<sup>5-6</sup>. The large effect of flow separation on inlet total pressure recovery and distortion is illustrated by the data of Figure 13 for the hard-wall diffuser and for an acoustically treated one. This figure indicates that flow separation produces a much larger change in inlet performance than does acoustic treatment. It is important therefore to determine if the angle of attack resulting in inlet flow separation is influenced by acoustic treatment.

The angle of attack at which flow separation occurred was determined by continuously monitoring pressures on the inlet lip and at the diffuser exit as angle of attack was increased. This technique is illustrated by the pressure traces of Figure 14 where flow separation can be identified by the rapid increase in total pressure distortion at the diffuser exit, Figure 14(a), and by the sharp increase in lip static pressure, Figure 14(b). The separation angle for this particular test sequence was approximately 42 degrees. Note that the traces indicate a substantial amount of hysteresis with flow re-attachment occurring at an angle well below the separation angle.

In Figure 15 the separation angle determined in the manner just described is shown as a function of average throat Mach number. The open symbols show data obtained with the acoustically treated diffusers while the solid symbols, connected by the dashed line, indicate the separation angles measured with the untreated hard-wall diffuser. The scatter band, obtained by repeatedly separating a number of the treated inlets, indicates the degree of nonrepeatability of the data due to the unsteady nature of flow separation. Repeated separation tests were not performed with the present hard-wall inlet. However, repeated tests of a similar hard-wall inlet also showed a scatter band. Within the limits imposed by this data scatter, no consistent effect of acoustical wall treatment on separation angle could be detected. This result indicates that acoustical treatment can be placed relatively far forward in an inlet, approaching the throat, without necessarily reducing the ability of the inlet to tolerate high angles of attack.

### Summary of Results

It was the purpose of the present investigation to determine experimentally the effect of diffuser wall acoustical treatment on inlet total pressure loss. The results presented were obtained by testing an inlet model with 10 different acoustically treated diffusers. All diffusers had the same contour and differed only in the design of the Helmholtz resonator type acoustic treatment. The major results of this investigation may be summarized as follows:

1. Pressure loss over the acoustic treatment was not influenced by the presence or absence of noise generated by a siren, even though the treatment attenuated the siren tone sound pressure level by as much as 8 dB. This indicates that the pressure loss in the boundary layer over the porous surface is great enough to mask any additional pressure loss generated as a result of exciting the Helmholtz resonators.
2. Inlet total pressure loss increased when acoustic treatment was added to the diffuser. For average throat Mach numbers of .5 to .7, the increase in pressure loss coefficient was found to be linearly proportional to the porosity of the acoustic treatment facing sheet and independent of throat Mach number. For example, acoustic treatment with a facing sheet porosity of 14 percent resulted in an increase in pressure loss of approximately 21 percent compared to the untreated inlet; whereas a penalty of 10 percent was measured for inlets with a porosity of 6.4 percent.
3. Inlet pressure loss was unaffected by changes in the depth of the honeycomb treatment for throat Mach numbers below .7.
4. The pressure loss coefficient increased for average throat Mach numbers above 0.7 with the untreated baseline inlet due to local regions of sonic or supersonic diffusing flow.
5. The increase in pressure loss coefficient chargeable to acoustic treatment was greatest for average throat Mach numbers above 0.7 indicating an additional penalty with acoustic treatment when placed in regions of locally sonic or supersonic flow.
6. The increase in inlet pressure loss and distortion due to angle of attack was not significantly affected by acoustic treatment. Additionally, diffuser acoustic treatment did not appear to alter the angle of attack resulting in inlet flow separation.

### Concluding Remarks

The results presented in this paper were obtained from tests of acoustically treated diffusers in a representatively contoured model inlet. A large number of total pressure measurements were averaged to obtain the effect of wall treatment on inlet pressure loss. Results show

pressure loss due to acoustic treatment to be influenced primarily by facing sheet porosity and grazing flow Mach number. For the present investigation facing sheet porosity was varied by changing the number of holes in the facing sheet. Porosity could also have been varied with a constant number of holes by simply changing hole diameter. The effect of this approach, and its influence on the results presented here, is not known and is an obvious area warranting further investigation.

An attempt was made, the results of which are not presented in this paper, to determine analytically the equivalent sand grain roughness corresponding to each acoustic treatment. The combined potential flow boundary layer program described by reference 7 was used to compute displacement thickness and momentum thickness at the diffuser exit as a function of sand grain roughness. This effort was only partially successful. Although it was found that an equivalent sand grain roughness could be found for each acoustic treatment that would fit the pressure loss data as a function of average throat Mach number, the analytically determined boundary layer profile at the diffuser exit did then not match well with the measured profile. That is, when the integrated total pressure loss for the two profiles were forced to agree, it was found that they differed substantially in shape.

Several factors may be responsible for, or contribute to, this apparent inconsistency. Firstly, sufficiently detailed boundary layer profiles may not have been measured during the tests. In keeping with the test objective, which was to determine the first order effects of treatment on inlet pressure loss and performance, relatively coarsely spaced, fixed position probes were used. Although this measurement technique is accepted as sufficient for determining inlet total pressure loss, it does not result in the detailed boundary layer profiles that could have been obtained with a small diameter, radially traversing probe. More detailed measurements may have altered the pressure loss sufficiently to result in better agreement between the experimental and theoretical boundary layer profiles. A second possible contributing factor may lie in the nature of the treated surface itself. The boundary layer generated as a result of flow over the porous plate may not develop with the same profile assumed by the analysis for a surface roughened with sand particles.

The need for more analytical work, combined with appropriate detailed measurement of boundary layer profiles, is clearly indicated in order to estimate with confidence the aerodynamic penalty likely to result from acoustic treatment. An analytical capability would greatly facilitate an investigation of such effects as model size or Reynolds number, grazing Mach number, diffusion rates, and treatment design on inlet performance.

### References

1. Feller, C. E. and Conrad, E. W., "Noise from Turbomachinery," AIAA Paper 73-815, St. Louis, Mo., 1973.
2. Bloomer, H. E. and Schaefer, J. W., "Aerodynamic and Acoustic Performance of a Contracting Cowl High Throat Mach Number Inlet Installed on NASA Quiet Engine C", AIAA Paper 76-540, Palo Alto, Calif., 1976.
3. Kazin, S. B. and Paas, J. E., "NASA/GE Quiet Engine A Acoustic Test Results", R73AEG 363, Oct. 1973, General Electric. Co.; also NASA CR-121175.
4. Boldman, D. R. and Brinich, D. F., "Skin Friction on a Flat Perforated Acoustic Liner", AIAA Journal, Nov. 1976.
5. Miller, B. A., Dastoli, B. J., and Wesoky, H. L., "Effect of Entry-Lip Design on Aerodynamics and Acoustics of High Throat-Mach-Number Inlets for the Quiet, Clean, Short-Haul Experimental Engine," TM X-3222, 1975, NASA.
6. Jakubowski, A. K., and Luidens, R. W., "Internal Cowl-Separation at High Incidence Angles," AIAA Paper 75-64, Pasadena, Calif., 1975.
7. Albers, J. A.; and Gregg, J. L., "A Computer Program to Calculate Laminar, Transitional, and Turbulent Boundary Layers for Compressible Axisymmetric Flow," TN D-7521, 1974, NASA.



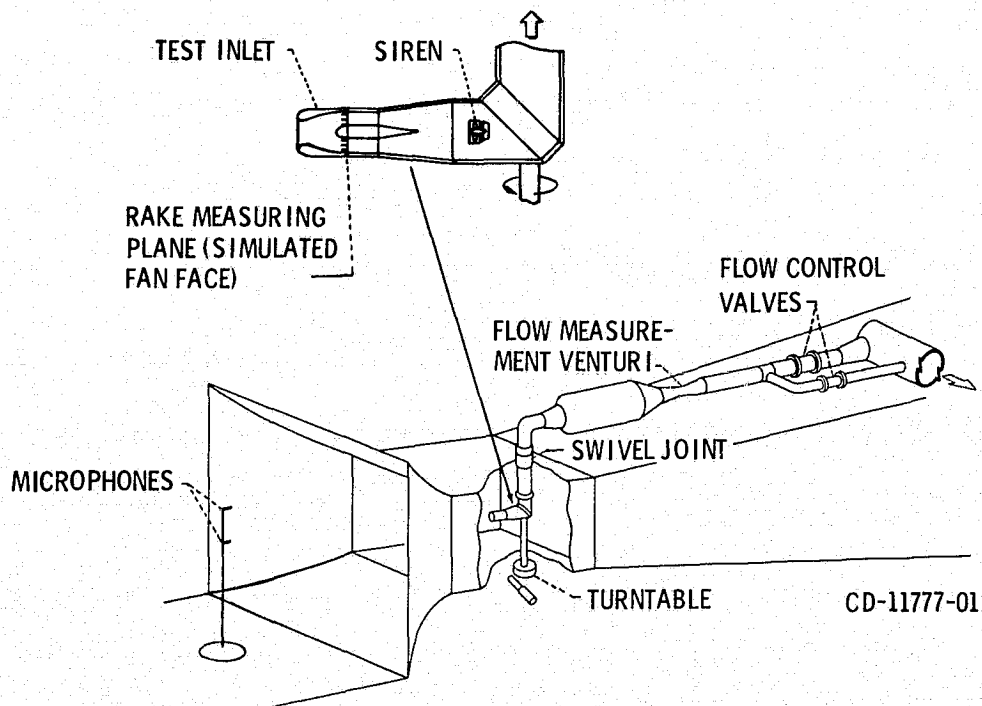
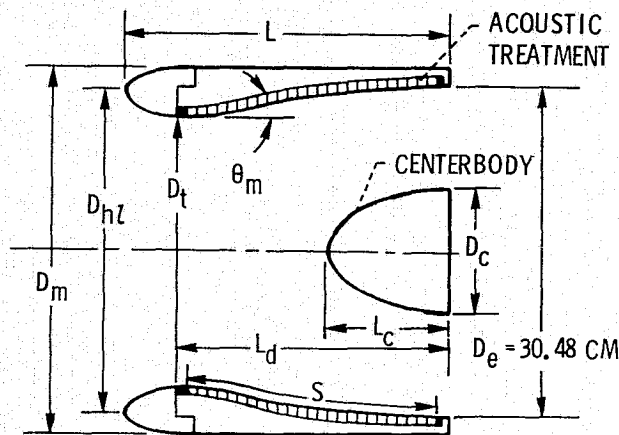


Figure 1. - Low speed wind tunnel showing model arrangement.



(a) DIFFUSER.

RATIO OF DIFFUSER LENGTH TO EXIT DIAMETER, $L_d/D_e$ . . . . .	0.875
RATIO OF TREATMENT LENGTH TO EXIT DIAMETER, $S/D_e$ . . . . .	.82
RATIO OF EXIT FLOW AREA TO INLET FLOW AREA, $(D_e^2 - D_c^2)/D_t^2$ . . . . .	1.093
MAXIMUM LOCAL WALL ANGLE, $\theta_m$ , DEG . . . . .	10.7
LOCATION OF MAXIMUM LOCAL WALL ANGLE, PERCENT $L_d$ FROM THROAT . . . . .	26.2
RATIO OF CENTERBODY DIAMETER TO DIFFUSER EXIT DIAMETER, $D_c/D_e$ . . . . .	0.4

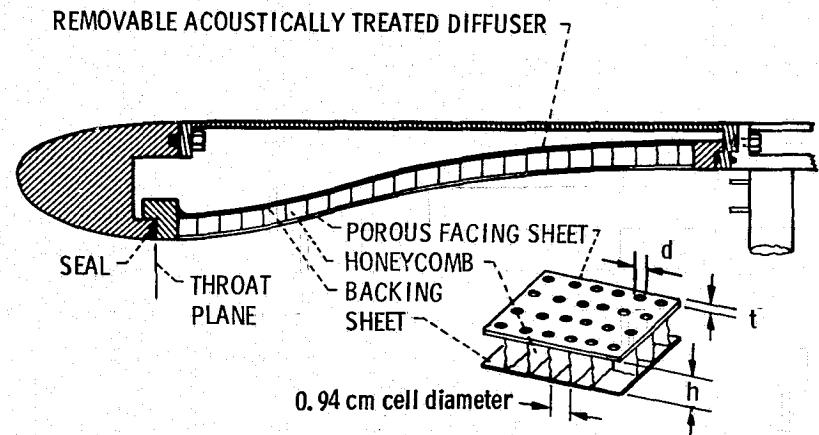
(b) CENTERBODY.

RATIO OF LENGTH TO DIAMETER, $L_c/D_c$ . . . . .	1.0
RATIO OF CENTERBODY LENGTH TO DIFFUSER LENGTH, $L_c/L_d$ . . . . .	.457

(c) ENTRY LIP.

INTERNAL LIP CONTRACTION RATIO, $(D_{hl}/D_t)^2$ . . . . .	1.34
EXTERNAL FOREBODY DIAMETER RATIO, $D_{hl}/D_m$ . . . . .	.846
RATIO OF OVERALL INLET LENGTH TO DIFFUSER EXIT DIAMETER, $L/D_e$ . . . . .	1.01

Figure 2 - Inlet nomenclature and summary of geometric variables.



TREATMENT DESIGNS TESTED

HOLE DIAMETER, $d$ , 0.114 cm FACING SHEET THICKNESS, $t$ , 0.05 cm	
FACING SHEET POROSITY, $\sigma$ , % $\sigma = N(\pi d^2/4) \times 100$ N = NUMBER OF HOLES PER UNIT AREA	HONEYCOMB DEPTH, $h/D_e$
2	.0075
2	.015
6.4	.0075
6.4	.015
6.4	.0275
9.6	.015
9.6	.0275
9.6	.0383
14	.0275
14	.0383

Figure 3. - Acoustic treatment design.

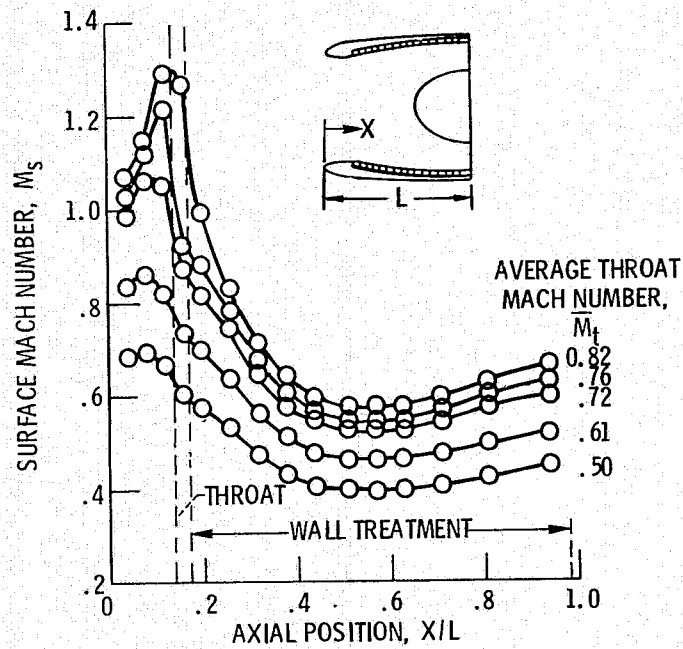


Figure 4. - Axial variation of surface Mach number as a function of average throat Mach number. Free stream velocity,  $V_0$ , 41 meters per second (80 knots); angle of attack,  $\alpha$ , 0 degrees.

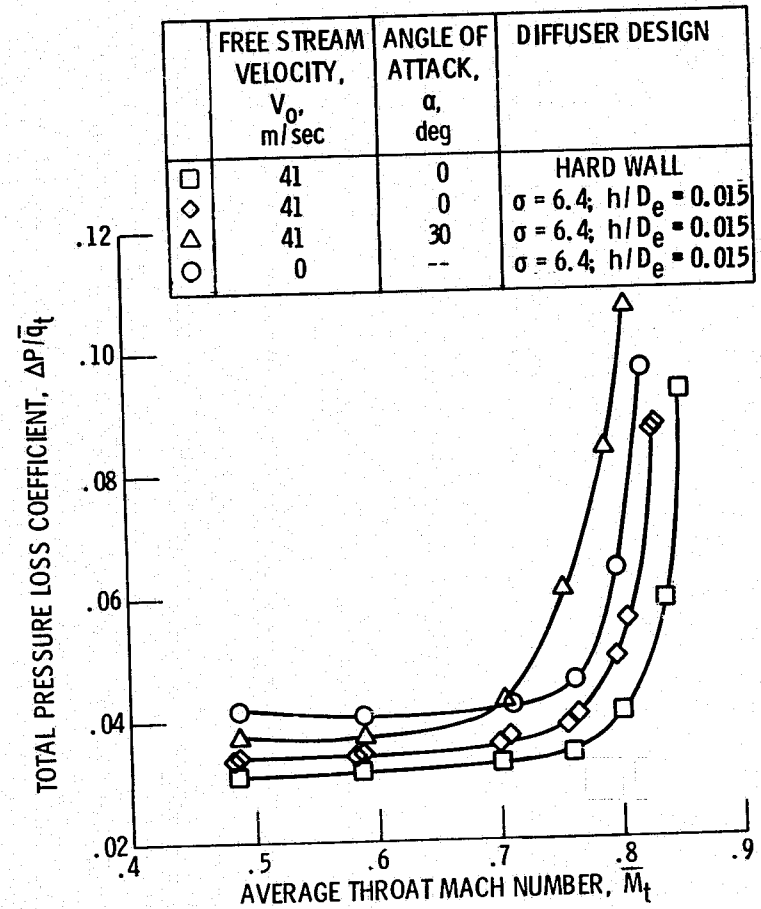


Figure 5. - Representative test results showing variation of total pressure loss with average throat Mach number for several operating conditions.

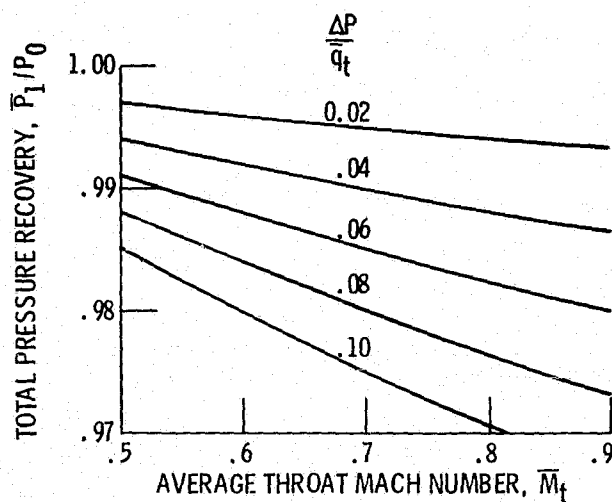


Figure 6. - Relation between total pressure loss coefficient and total pressure recovery as a function of average throat Mach number.

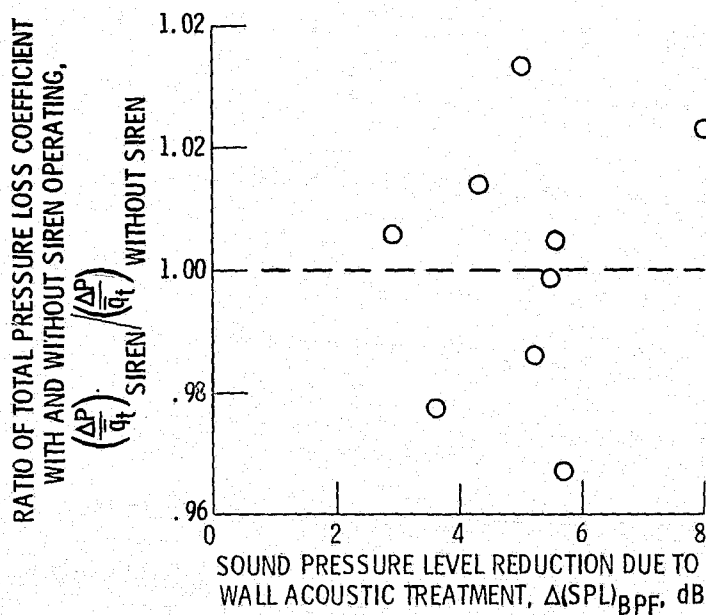


Figure 7. - Comparison of total pressure loss with and without impressed noise. Each data point obtained with a different treatment by averaging the results at throat Mach numbers of 0.5 to 0.7 with a free stream velocity of 41 meters per second (80 knots) and 0 degree angle of attack. Siren blade passing frequency, 5000 Hz.

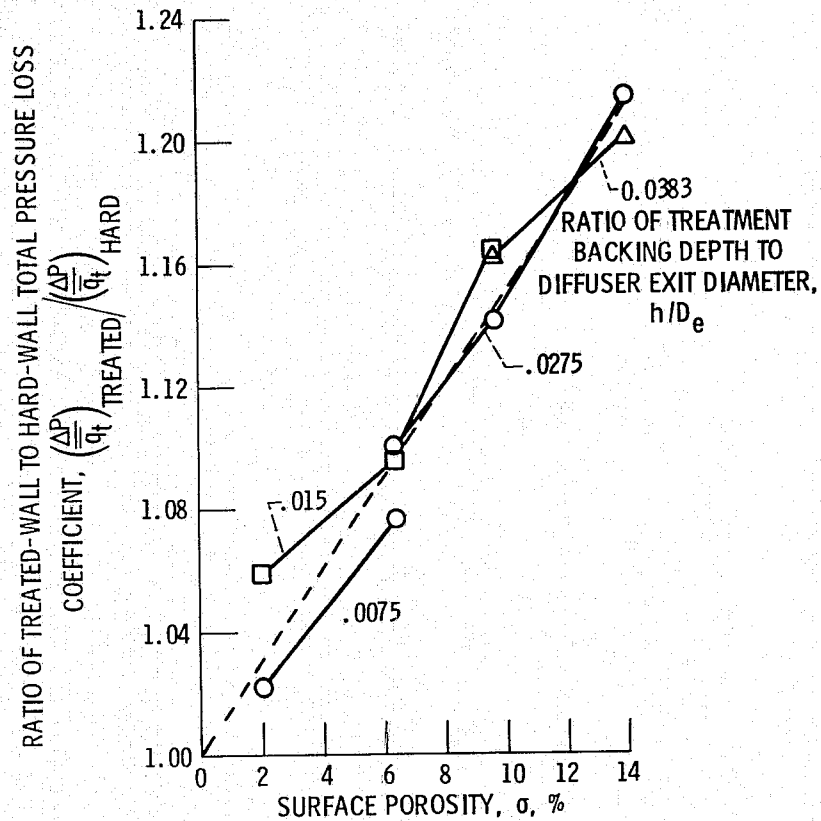


Figure 8. - Increase in total pressure loss due to wall treatment surface porosity. Results obtained by averaging losses for average throat Mach numbers of 0.5 to 0.7 at a free stream velocity of 41 meters per second (80 knots) and 0 degrees angle of attack.

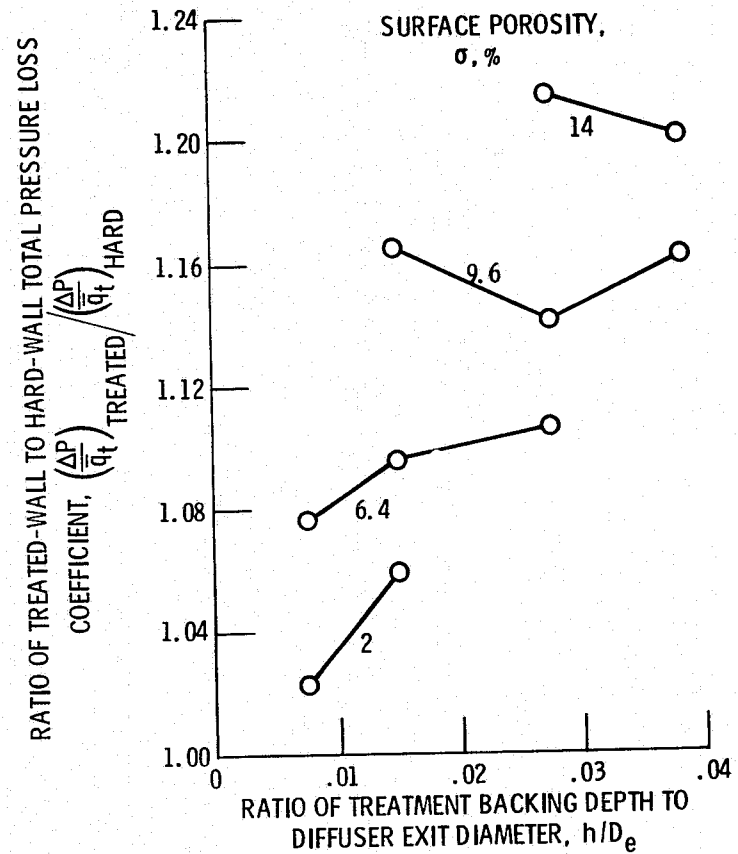
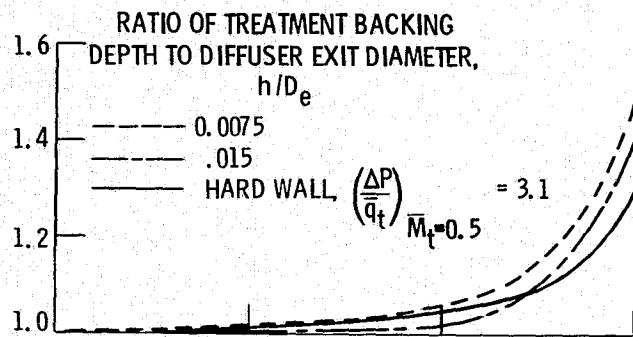
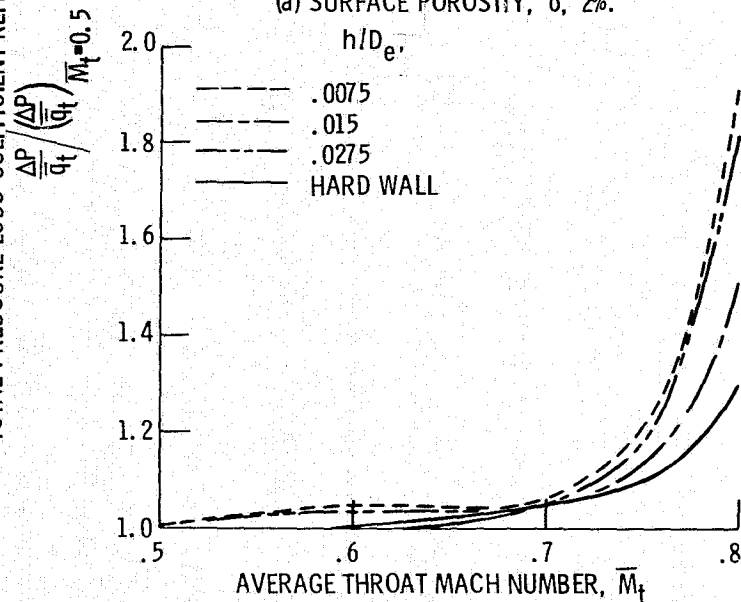


Figure 9. - Effect of treatment backing depth on total pressure loss. Results obtained by averaging losses for average throat Mach numbers of 0.5 to 0.7 at a free-stream velocity of 41 meters per second (80 knots) and 0 degree angle of attack.

TOTAL PRESSURE LOSS COEFFICIENT REFERENCED TO  $\bar{M}_t = 0.5$ ,

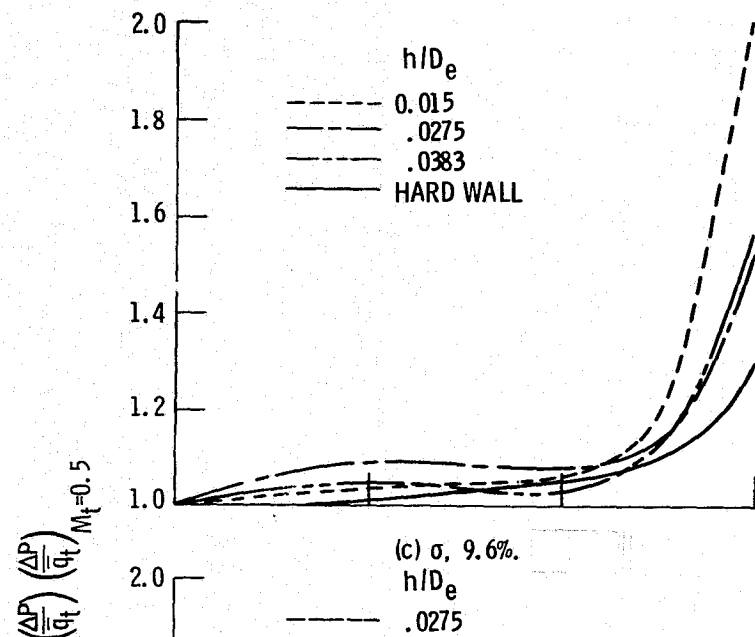


(a) SURFACE POROSITY,  $\sigma$ , 2%.

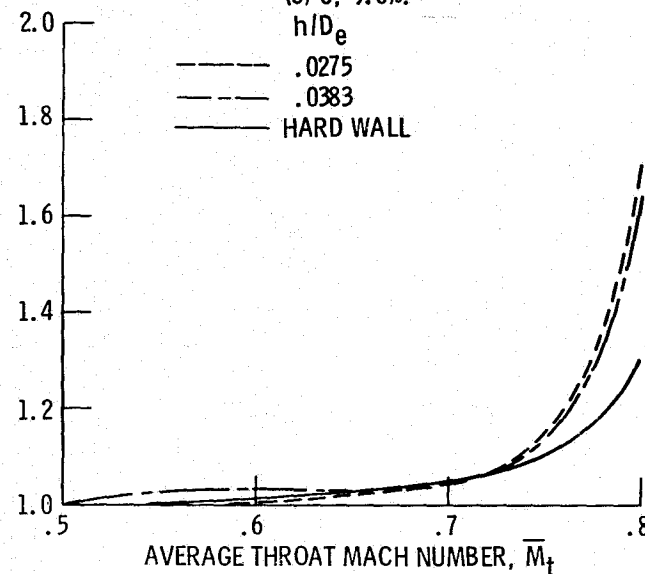


(b)  $\sigma$ , 6.4%.

Figure 10. - Increase in total pressure loss coefficient with increasing average throat Mach number. Free stream velocity,  $V_0$ , 41 meters per second (80 knots); angle of attack,  $\alpha$ , 0 degree.



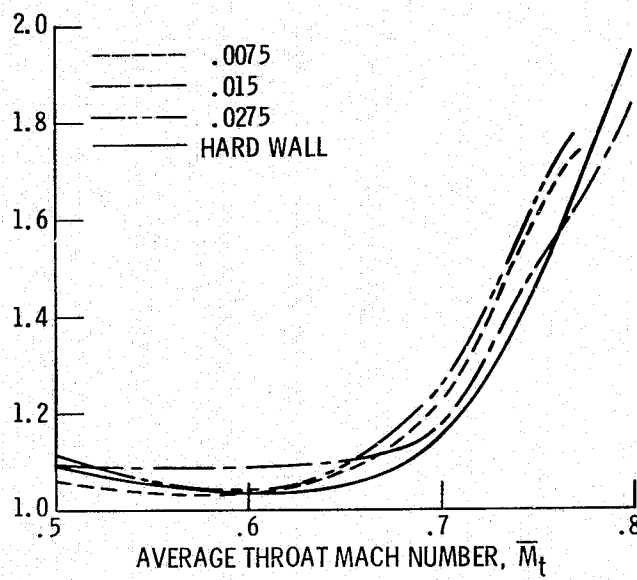
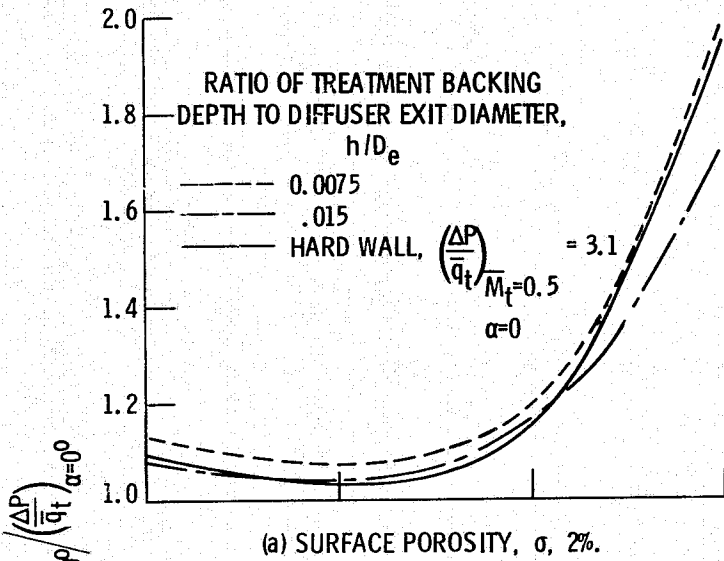
(c)  $\sigma$ , 9.6%.



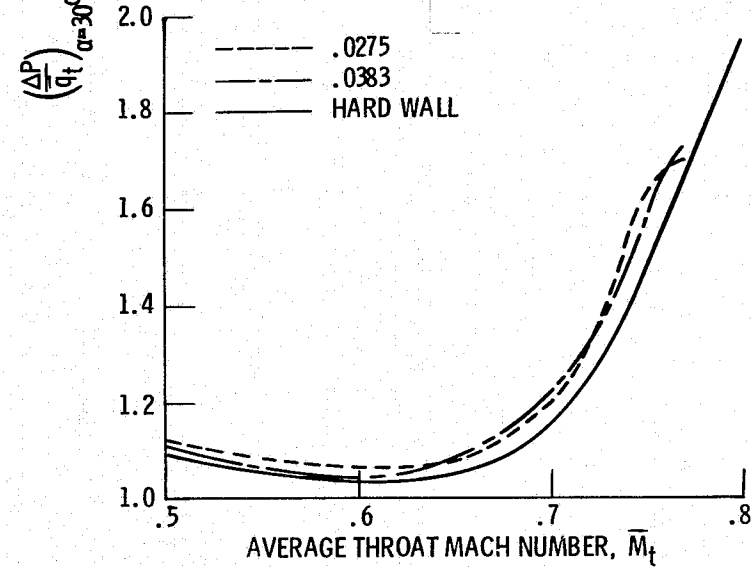
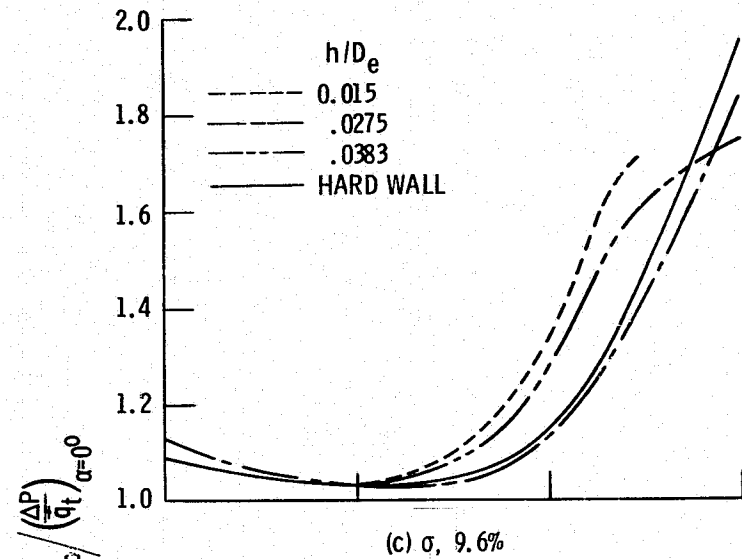
(d)  $\sigma$ , 14%.

Figure 10. - Concluded.

RATIO OF TOTAL PRESSURE LOSS AT 30 DEGREES ANGLE OF ATTACK TO PRESSURE LOSS AT 0 DEGREES



(b)  $\sigma$ , 6.4%.



(d)  $\sigma$ , 14%.

Figure 11. - Increase in total pressure loss at 30 degrees angle of attack compared to 0 degrees. Free stream velocity,  $V_\infty$ , 41 meters per second (80 knots).

Figure 11. - Concluded.

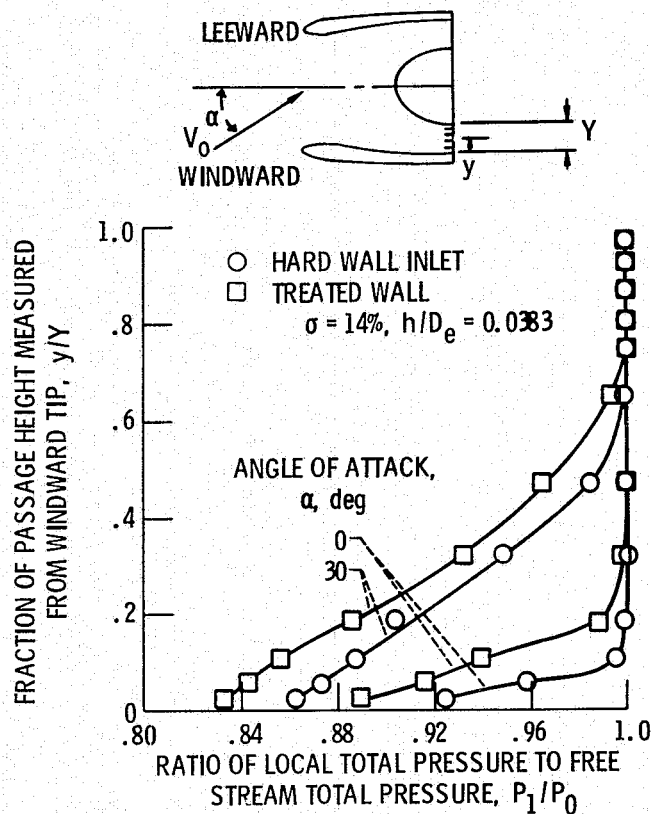


Figure 12. - Representative effect of angle of attack and acoustic treatment on diffuser exit total pressure profiles. Free stream velocity,  $V_0$ , 41 meters per second (80 knots); average throat Mach number,  $\bar{M}_t$ , 0.80.

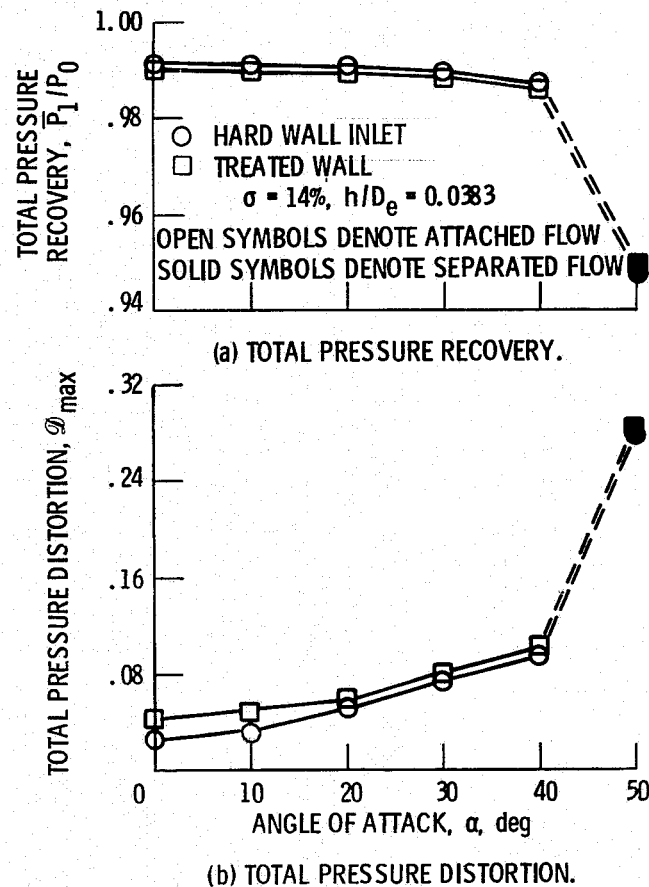
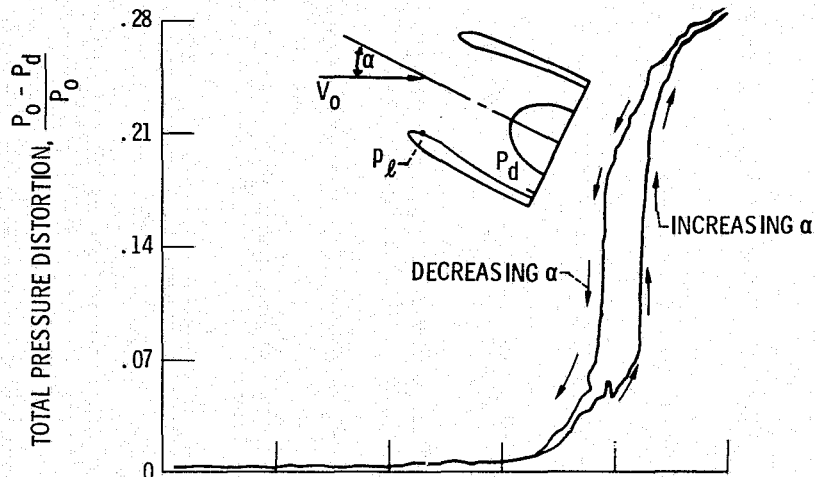
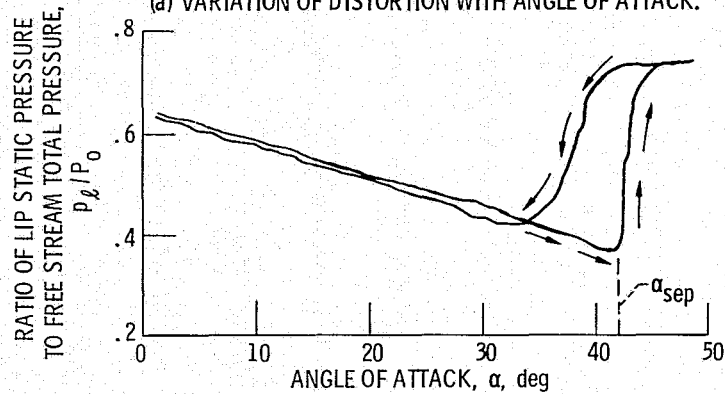


Figure 13. - Representative effect of angle of attack on total pressure recovery and distortion. Free stream velocity,  $V_0$ , 41 meters per second (80 knots); average throat Mach number,  $\bar{M}_t$ , 0.7 to 0.72.





(a) VARIATION OF DISTORTION WITH ANGLE OF ATTACK.



(b) VARIATION OF LIP STATIC PRESSURE WITH ANGLE OF ATTACK.

Figure 14. - Typical data used to detect flow separation at constant free stream velocity and average throat Mach number.

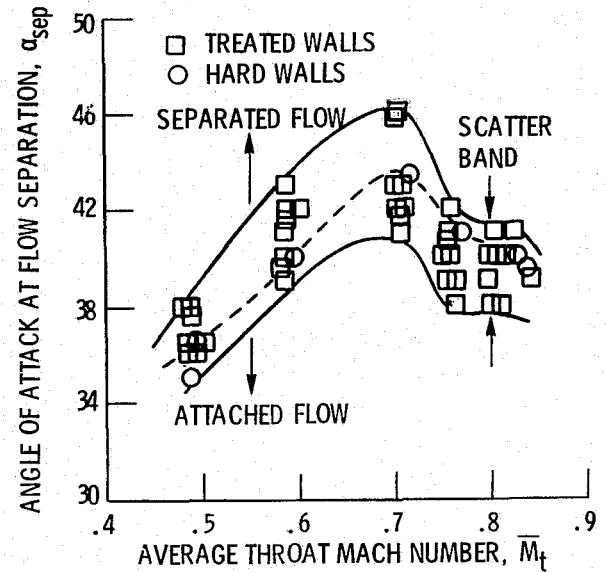


Figure 15. - Effect of wall treatment and average throat Mach number on separation angle.